

Ultralow dielectric constant nickel–zinc ferrites using microwave sintering

Ramesh Peelamedu,^{a)} Craig Grimes, Dinesh Agrawal, and Rustum Roy

Materials Research Institute, The Pennsylvania State University, University Park, Pennsylvania 16802

Purushotham Yadoji

Centre for Materials for Electronics Technology (C-MET), Cherlapally, HCL(PO), Hyderabad, 500 051, India

(Received 21 May 2003; accepted 21 July 2003)

Ultralow dielectric constant values were measured on Ni–Zn ferrites prepared using Fe_2O_3 as a starting material and sintered in a microwave field. Significant differences in microstructure, magnetic, and dielectric properties were observed between microwave-sintered Ni–Zn ferrites prepared using Fe_3O_4 (T34) and those starting with Fe_2O_3 (T23) ingredients. Higher magnetization values observed in T23 ferrite are attributed to large grain size, possibly containing abundant domain walls and the presence of fewer Fe^{2+} ions. The ultralow dielectric constant values observed on T23 ferrites show that this procedure is highly suitable to prepare Ni–Zn ferrites for high-frequency switching applications.

Nickel–zinc ferrites are very important soft magnetic materials that have many applications in both low- and high-frequency devices and play a useful role in many technological applications because of their high resistivity, low-dielectric loss, mechanical hardness, high Curie temperature, and chemical stability.^{1–3} Microstructure, magnetic, and dielectric properties of Ni–Zn ferrites depend on the method of preparation, sintering conditions, and the doping concentration. The selection of an appropriate process is essential in obtaining good-quality ferrites. Ni–Zn ferrites are usually prepared by the conventional ceramic procedure that involves direct mixing of the constituent oxides radiant-heated in a conventional furnace. Prolonged heating at high temperatures is partly disadvantageous as it involves volatilization of some constituents and results in a nonstoichiometric product. The advantages of microwave processing for ceramics have been described in a series of papers from this and other laboratories.^{4–6} While using mixtures of oxides involving $3d$ ions, differences in absorption among the constituent phases lead to “anisothermal effect,” which is possible only in the microwave procedure. Ni–Zn ferrites prepared by different methods such as combustion, hydrothermal, citrate, and sol-gel methods exhibit dissimilar dielectric and magnetic properties. Recently, the authors have demonstrated that the microwave and conventionally prepared nickel–zinc ferrites exhibit different

dielectric and magnetic properties.⁷ Also, there is hardly any report featuring the effect of microwave sintering on the magnetic and dielectric properties of ferrite material sintered using Fe_2O_3 and Fe_3O_4 .

In this paper, a systematic investigation of Ni–Zn ferrites prepared using Fe_3O_4 (T34) and Fe_2O_3 (T23) as starting powders and their sintering under the influence of microwave energy is described. The effects of starting powder on various properties such as density, microstructure, and magnetic and dielectric studies are presented.

$\text{Ni}_{1-x}\text{Zn}_x\text{Fe}_2\text{O}_4$ with $0 \leq x \leq 1$ was prepared using high-purity NiO, ZnO, and $\text{Fe}_3\text{O}_4/\text{Fe}_2\text{O}_3$ in stoichiometric proportions. The powders, after thorough mixing and grinding, were calcined at 1100 °C for 4 h in a conventional furnace. All compositions were sintered at 1275 °C for 30 min using a multimode microwave furnace (2.45 GHz) (Amana Radarange, Model RC/20SE, Amana Refrigeration Inc., Amana, IA) operating at a maximum input power of 2.0 kW (the output power of magnetron is roughly 50–60% on the input power). A detailed description of the setup and related details can be found elsewhere.⁶ At least three samples in each composition were placed at the center of the tube, where the microwave flux was maximum. Despite the fact that Ni–Zn ferrites are very good microwave absorbers, preliminary experiments showed that the thermal runaway caused stress-induced cracks throughout the sample. To prevent this problem, the samples were placed on a thin SiC plate that also acted as a preheater. Modeling results established the fact that the SiC plates, in addition to the thermal support, also help in focusing the

^{a)}Address all correspondence to this author.
e-mail: rdp10@psu.edu

electromagnetic field around the sample.⁷ In our experiments, the emissivity of the single-wavelength infrared pyrometer was set at $e = 0.75$, and this value was chosen by calibrating against the optical pyrometer set at the other side of the tube.⁸ All sintered samples were characterized using x-ray diffraction (XRD) (Scintag Inc., Cupertino, CA). Sintered densities were measured by the Archimedes method (Table I) whereas microstructures were examined using scanning electron microscopy (SEM) (Hitachi Ltd., Tokyo, Japan). The magnetic measurements were carried out using a vibrating sample magnetometer (Lakeshore Cryotronics Inc., SHB Model 109, SHB Instruments Inc., Northridge, CA) and dielectric properties were measured by an impedance analyzer (Model 4194A, Hewlett Packard, Tokyo, Japan) in the frequency range from 1 kHz to 13 MHz.

Ni–Zn ferrite is a mixed normal-inverse spinel type with a general formula $\text{Fe}_{1-x}\text{Zn}_x(\text{Ni}_{1-x}\text{Fe}_{1+x})\text{O}_4$. The substitution of Ni^{2+} by diamagnetic Zn^{2+} ions produces a mixed effect on the magnetic properties. In NiFe_2O_4 , the divalent metal ions occupying the octahedral sites (B) and the trivalent Fe ions are distributed among tetrahedral (A) and the octahedral sites (B). On the other hand, ZnFe_2O_4 has a spinel structure with Zn^{2+} ions occupying A sites and Fe^{3+} occupying B sites. Because Zn^{2+} (d^{10}) has a site preference for A sites, with more and more Zn^{2+} replacing Ni^{2+} , the spin–spin interaction between nonmagnetic Zn^{2+} and Fe^{3+} ions becomes increasingly uncoupled. This uncoupling effect with composition is reflected in the magnetization graph. The M – H curves measured for T34 and T23 ferrites are shown in Fig. 1. The magnetic moment (μ_B) per atom in Bohr magneton for each composition is calculated using the experimental values of saturation magnetization (M_s) and the equation,

$$\mu_B = \frac{M \times M_s}{N \times \beta} \quad (1)$$

where M is the molecular weight of the specimen, N is Avagadro's number, and β is the conversion factor to express the magnetic moment per atom in Bohr magnetons (its value is 9.27×10^{-21} erg/gauss). In Fig. 2, we see an increase in Bohr magneton value up to $x = 0.4$ in the case of type-34 and up to $x = 0.6$ in the case of

type-23 ferrites. Further increasing Zn substitution will make the material increasingly diamagnetic, which leads to a decrease in Bohr magneton values.

It is reported that in the conventional Ni–Zn ferrites processing procedure, Fe^{2+} ions are believed to be introduced due to the following reasons: (i) volatilization of zinc atoms and (ii) oxidation/reduction (heating/cooling cycles). In the case of the microwave procedure, however, an electromagnetic field effect exists in addition to the usual heat transfer effects. The microwave magnetic field effect on sublattice disordering has been well established in our other publications.⁹ Despite the fact that the sublattice disordering effect has been well established in a single-mode microwave field, any such strong

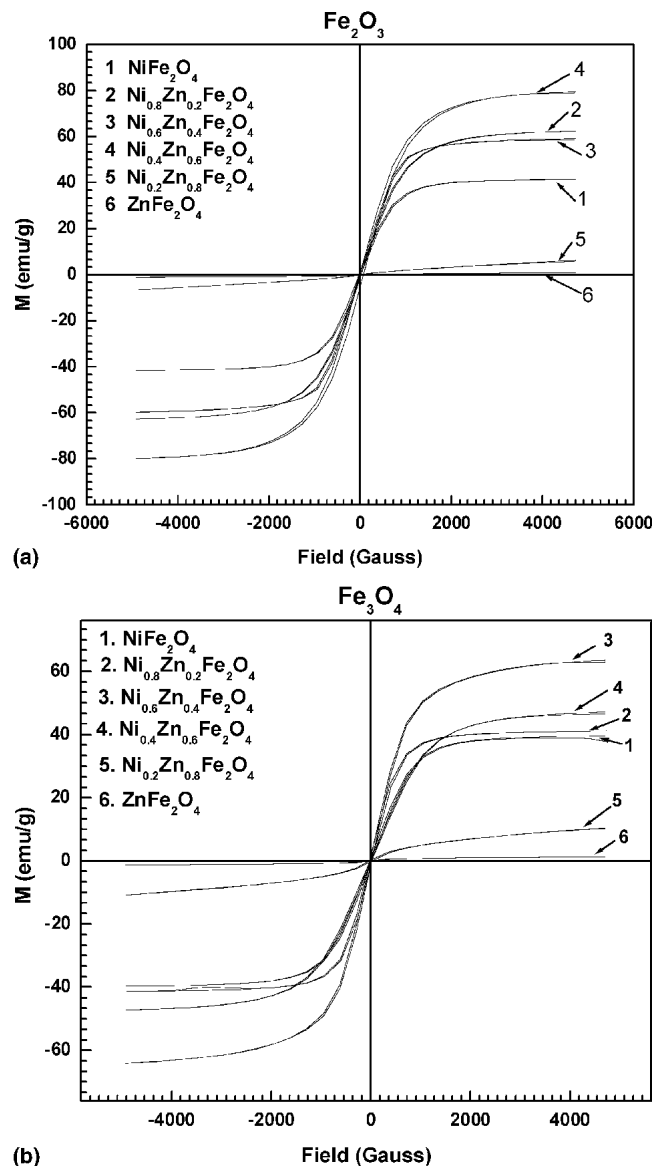


FIG. 1. Room temperature M – H graphs of Ni–Zn ferrites sintered at 1275 °C for 30 min: (a) prepared using Fe_2O_3 powder; (b) prepared using Fe_3O_4 powder.

TABLE I. Densities of type-23 and type-34 ferrites sintered at 1275 °C for 30 min in a microwave field.

Sample	Composition	Type-23 density (kg/m ³)	Type-34 density (kg/m ³)
NZF-1	NiFe_2O_4	5.09	5.09
NZF-2	$\text{Ni}_{0.8}\text{Zn}_{0.2}\text{Fe}_2\text{O}_4$	5.07	4.96
NZF-3	$\text{Ni}_{0.6}\text{Zn}_{0.4}\text{Fe}_2\text{O}_4$	5.04	4.99
NZF-4	$\text{Ni}_{0.4}\text{Zn}_{0.6}\text{Fe}_2\text{O}_4$	5.01	5.04
NZF-5	$\text{Ni}_{0.2}\text{Zn}_{0.8}\text{Fe}_2\text{O}_4$	4.97	5.05
NZF-6	ZnFe_2O_4	4.96	4.87

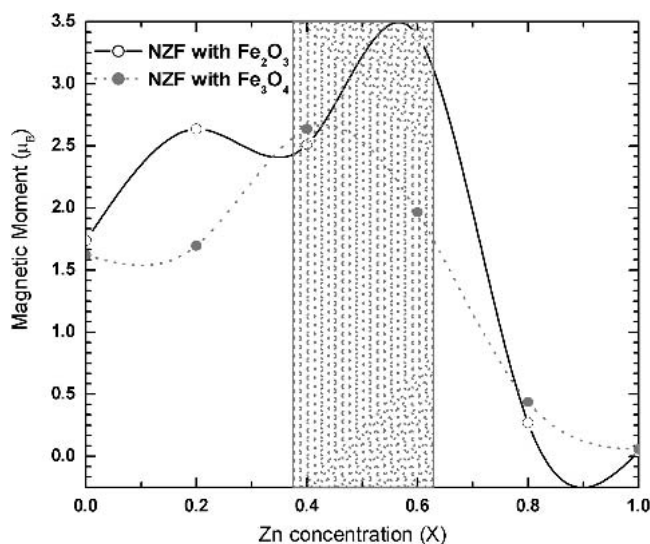


FIG. 2. Variation of Bohr magneton with zinc addition in Ni-Zn ferrites.

effects in a multimode cavity is unclear.¹⁰ The results reported in this paper clearly indicate that at least the charged cations interact to a limited extent to create a finite, nonzero disorder locally, which can significantly alter the magnetic properties. Because the sintering temperatures and heating and cooling cycles were identical for T34 and T23 ferrites, the significant differences in Bohr magneton values could have arisen from the local sublattice nonstoichiometries. At this point, the exact nature of such interactions are only hypothetical and are being studied.⁸

Microstructural comparisons between T34 and T23 materials are depicted in Fig. 3. The SEM micrograph of T34 material reveals circular pores narrowly distributed, spread throughout the entire microstructure whereas irregular-shaped circular pores are more common in the case of T23 microstructure.

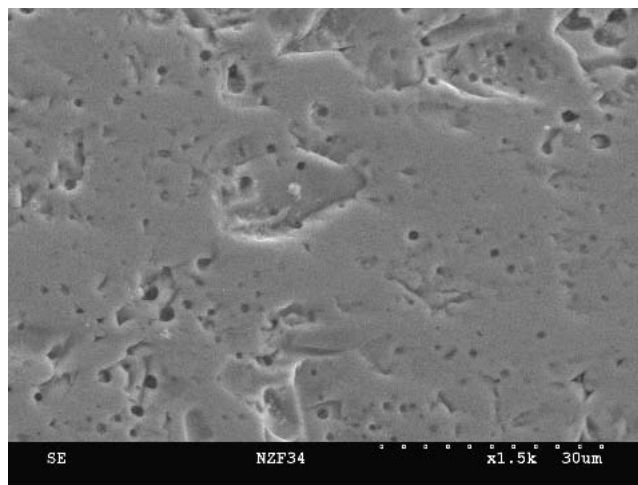
The grain-grain boundary morphology of a polycrystalline ferrite ceramic is analogous to an electrical circuit (resistor and capacitor connected parallel) connected in series. Let x be the ratio of the grain boundary to grain thickness and ρ_1 , ρ_2 , ϵ_1 , and ϵ_2 denote the resistivities and the relative dielectric constants of grain boundary and grain, respectively. If $x \ll 1$, $\epsilon_1 = \epsilon_2$, and $\rho_1 \gg \rho_2$. Then, the equations for resistivity and dielectric constant of the combined system can be written as:¹¹

$$\rho_p^\infty = \rho_2 \quad , \quad (2)$$

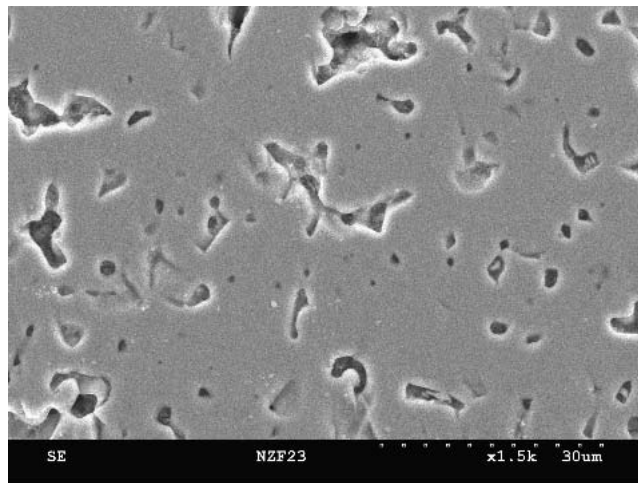
$$\rho_p^0 = x\rho_1 + \rho_2 \quad , \quad (3)$$

$$\epsilon_p^\infty = \epsilon_2 \quad , \quad (4)$$

$$\epsilon_p^0 = \epsilon_2 \times \frac{x\rho_1^2 + \rho_2^2}{(x\rho_1 + \rho_2)^2} \quad . \quad (5)$$



(a)



(b)

FIG. 3. SEM micrographs of microwave-sintered Ni-Zn ferrites prepared using (a) Fe_3O_4 and (b) Fe_2O_3 .

In these equations, ρ_p^∞ and ϵ_p^∞ correspond to resistivity and relative dielectric constant at higher frequencies and ρ_p^0 and ϵ_p^0 correspond to the same values at low frequencies, respectively. From these equations, it is important to note that at higher frequencies, the bulk resistivity approaches that of grain resistivity and its dielectric constant value. The frequency effect on dielectric constant values for T34 and T23 ferrites are illustrated in Fig. 4. For T34 material, the maximum value of dielectric constant is 2483 for NiFe_2O_4 at 1 kHz; whereas this value is just 12 for T23 material. The dielectric constant value of all other T23 compositions is only of the order of a few tens. Starting from low frequency, the curve decreases sharply, and the decreasing trend becomes increasingly slower at higher frequencies. This decreasing trend at higher frequencies can be explained by the

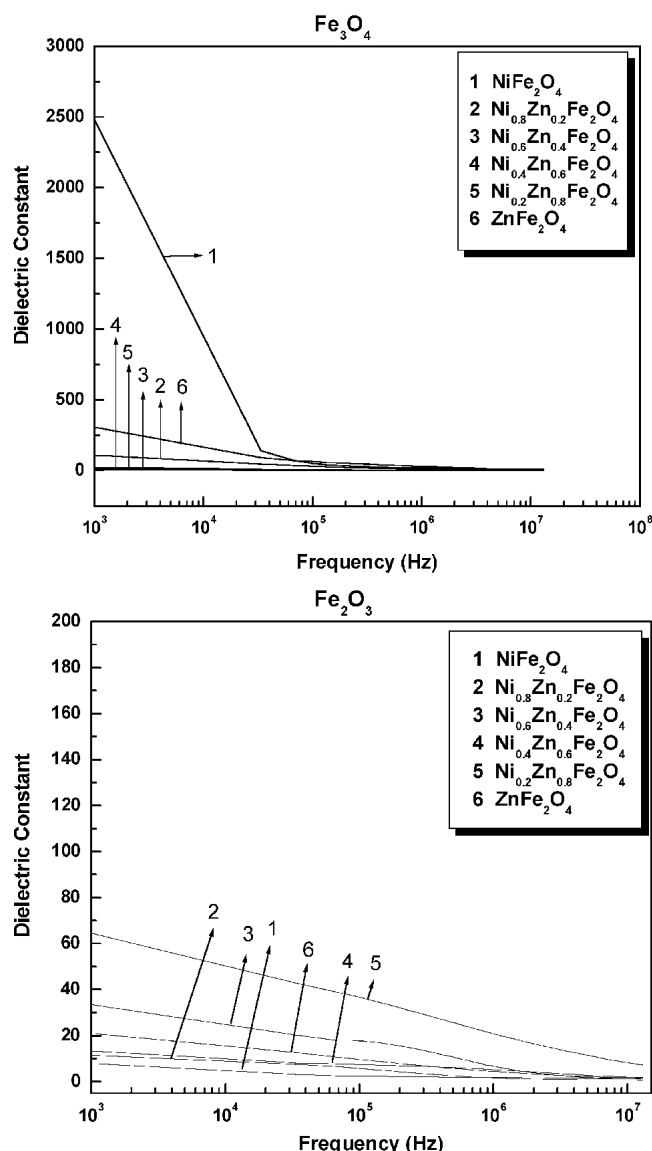


FIG. 4. Dielectric constant variation with frequency for microwave-sintered Ni–Zn ferrites prepared using Fe_3O_4 (type 34) and Fe_2O_3 (type 23). The type-23 ferrites show low values of dielectric constant compared to type-34 ferrites.

Maxwell–Wagner theory. The relationship between dielectric constant (ϵ'), frequency (f), electrical conductivity (σ'_{AC}), and loss factor ($\tan \delta$) can be written as

$$\epsilon' = \frac{4\pi\sigma'_{AC}}{[2\pi f \tan \delta]} \quad (6)$$

where both ϵ' and $\tan \delta$ are inversely proportional with frequency.^{12,13} The dielectric constant values obtained in this study with Fe_2O_3 precursor appear lower than any other method for all Ni–Zn compositions (which

generally are in the range of 10^2 to 10^5).^{12–14} This value for pure NiFe_2O_4 , $\text{Ni}_{0.2}\text{Zn}_{0.8}\text{Fe}_2\text{O}_4$, and pure ZnFe_2O_4 is at least ten or more times lower than that of Ni–Zn ferrites produced by using Fe_3O_4 precursor. In other cases, these values are comparable. Nevertheless, these values are extremely lower compared to conventionally sintered nickel–zinc ferrites of all compositions prepared and measured in our own laboratory.⁸ Lower dielectric constants can arise from various factors such as (i) low concentration of Fe^{2+} ions that enables insufficient polarization when field is applied and (ii) lower density and higher porosity. Only the first point appears to be more suitable for T23 ferrite compared to T34. This means that the charged species in T23 and T34 respond quite differently under the influence of microwave electromagnetic field. The maximum value of dielectric loss (not shown) observed in the case of T34 is 25 and the maximum tangent loss value in the case of T23 material is about 40, which are quite comparable to the values reported for conventionally processed Ni–Zn ferrites.¹²

ACKNOWLEDGMENTS

One of the authors, Dr. Purushotham Yadoji, wishes to thank the Department of Science and Technology (India) for awarding a Better Opportunities for Young Scientists in Chosen Areas of Science and Technology (BOYSCAST) fellowship. The authors acknowledge Defense Advanced Research Projects Agency (DARPA) support for such microwave science at Materials Research Laboratory (MRL) via Grant No. N00014-981-1-0752.

REFERENCES

1. H. Igarashi and K. Okazaki, *J. Am. Ceram. Soc.* **60**, 51 (1977).
2. T. Abraham, *Am. Ceram. Soc. Bull.* **73**, 62 (1994).
3. P.I. Slick, in *Ferromagnetic Materials*, edited by E.P. Wohlforth (North-Holland, Amsterdam, The Netherlands, 1980), Vol. 2, p. 189.
4. K.J. Rao and P.D. Ramesh, *Bull. Mater. Sci.* **18**, 447 (1995).
5. R.D. Peelamedu, R. Roy, and D. Agrawal, *Mater. Res. Bull.* **36**, 2723 (2001).
6. R.D. Peelamedu, R. Roy, and D.K. Agrawal, *Mater. Lett.* **55**, 234 (2002).
7. M.F. Iskander, *MRS Bull.* **18**, 30 (1993).
8. P. Yadoji, R. Peelamedu, D. Agrawal, and R. Roy, *Mater. Sci. Eng. B* **98**, 269 (2003).
9. R. Roy, R. Peelamedu, C. Grimes, J. Cheng, and D. Agrawal, *J. Mater. Res.* **17**, 3008 (2002).
10. R. Roy, R. Peelamedu, L. Hurtt, J.P. Cheng, and D. Agrawal, *Mater. Res. Innov.* **6**, 128 (2002).
11. C.G. Koops, *Phys. Rev.* **83**, 121 (1951).
12. A.M. Abdeen, *J. Magn. Magn. Mater.* **192**, 121 (1999).
13. M.A. El Hiti, *J. Magn. Magn. Mater.* **192**, 305 (1999).
14. R.V. Mangala Raja, S. Anantha Kumar, P. Manohar, and F.D. Gnanam, *Mater. Lett.* **57**, 1151 (2003).